American Mineralogist, Volume 97, pages 568–572, 2012

High-pressure and high-temperature phase transitions in $FeTiO_3$ and a new dense $FeTi_3O_7$ structure

Daisuke Nishio-Hamane,[1,*] Meiguang Zhang,[2] Takehiko Yagi,[1] and Yanming Ma[2]

[1]Institute for Solid State Physics, the University of Tokyo, 5-1-5 Kashiwanoha, Kashiwa 277-8581, Japan
[2]State Key Lab of Superhard Materials, Jilin University, Changchun 130012, China

Abstract

High-pressure and high-temperature phase relations of $FeTiO_3$ were investigated up to a pressure of about 74 GPa and 2600 K by synchrotron X-ray diffraction and analytical transmission electron microscopy. We conclude that $FeTiO_3$ ilmenite transforms into the following phase(s) with increasing pressure: $FeTiO_3$ (perovskite) at 20–30 GPa, Fe_2TiO_4 (Ca_2TiO_4-type) + TiO_2 (OI-type) at 30–44 GPa and high temperature, FeO (wüstite) + TiO_2 (OI) at 30–44 GPa and low temperature, and wüstite + $FeTi_3O_7$ (orthorhombic phase) above 44 GPa. Among these dense high-pressure polymorphs, $FeTi_3O_7$ is a new compound and its structure analysis was tried using particle swarm optimization simulation. This method successfully found a new high-density $FeTi_3O_7$ structure, and Rietveld refinement based on this model structure gave an excellent fit with the experimentally obtained X-ray diffraction pattern. This new high-density $FeTi_3O_7$ structure consists of polyhedra for monocapped FeO_7 prisms, bicapped TiO_8 prisms, and tricapped TiO_9 prisms, which develop on the **b-c** plane and stack along the **a** axis. The dense compound assemblage found in $FeTiO_3$ is promising for investigating the behavior of ABX_3 compounds under ultrahigh pressures.

Keywords: $FeTiO_3$, $FeTi_3O_7$, high pressure, diamond-anvil cell

Introduction

Many ABX_3 compounds crystallize in the perovskite structure or some distorted derivative of it and they represent an important class of materials in physics, materials science, and Earth science. Due to its close-packed structure, the perovskite structure is stable over a wide range of pressures. However, it becomes unstable and transforms into denser structures at very high pressures. The discovery of the structural phase transition of perovskite into a $CaIrO_3$-type phase at high pressures (Murakami et al. 2004; Oganov and Ono 2004) stimulates the investigation of further phase transitions and close-packed structures in ABX_3 at high pressures, which is of fundamental interest in Earth science, mineralogy, and crystallography. Experimental and theoretical studies have suggested several sesquisulfide structures as high-pressure forms of post-$CaIrO_3$ structures (Umemoto and Wenzcovitch 2008; Yusa et al. 2008; Nishio-Hamane et al. 2009). Theoretical calculations based on density functional theory also predict several potential structures with ABX_3 stoichiometry and eventual decomposition into a assemblage of simple compounds ($ABX_3 \rightarrow AX + BX_2$) at ultrahigh pressures (Umemoto et al. 2006a; Umemoto and Wenzcovitch 2006; Tsuchiya and Tsuchiya 2011). On the other hand, recent experimental studies have detected a new dissociation of ABX_3 to a dense compound assemblage at high pressures (Nishio-Hamane et al. 2010b; Okada et al. 2011), namely $ABX_3 \rightarrow 2/3AX + 1/3AB_3X_7$ and $1/2AX + 1/2AB_2X_5$ for $FeTiO_3$ and $MnTiO_3$, respectively. In the case of $FeTiO_3$ (Nishio-Hamane et al. 2010b), its dissociation product was denser than the $CaIrO_3$ structure and an assemblage of wüstite FeO and cotunnite TiO_2 predicted by a theoretical study (Wilson et al. 2005), although an assemblage of AX and cotunnite-type BX_2 has often been predicted to be the terminal state for ABX_3 compounds at ultrahigh pressures. A phase assemblage denser than $AX + BX_2$ has not been considered, so far. Therefore, the phase relation of $FeTiO_3$ is expected to be significant for estimating the ultrahigh-pressure behavior of ABX_3 compounds such as $MgSiO_3$ and $CaSiO_3$, which may be a major component of the deep interiors of giant planets.

During compression at room temperature, $FeTiO_3$ ilmenite transforms into the perovskite phase at about 20 GPa; this perovskite phase has been observed up to pressures of about 50 GPa (Wu et al. 2009a, 2009b). However, when the metastable lithium niobate phase, which was formed by the retrogressive transition from perovskite phase on release of pressure, was used as a starting material, the perovskite phase stabilized above about 16 GPa (Leinenweber et al. 1991). Theoretical calculations at 0 K predict that the $CaIrO_3$ polymorph will form at 40 GPa and that it will dissociate into wüstite and cotunnite TiO_2 above 65 GPa (Wilson et al. 2005). In their experimental study, Wu et al. (2009b) claimed that perovskite dissociated to wüstite and a Ti-rich phase above 40 GPa by heating, and the Ti-rich phase was identified as $FeTi_2O_5$ with monoclinic symmetry. We have conducted TEM experiments on the recovered sample of our experiment and concluded that the Ti-rich phase is orthorhombic $FeTi_3O_7$ rather than monoclinic $FeTi_2O_5$ (Nishio-Hamane et al. 2010b). We further clarified that wüstite and the orthorhombic $FeTi_3O_7$ phase assemblage was stable even at about 70 GPa after heating to 2000 K. During this work, we have noticed the existence of some intermediate phases. Moreover, the structure of the orthorhombic $FeTi_3O_7$ phase has not been determined yet.

* E-mail: hamane@issp.u-tokyo.ac.jp

0003-004X/12/0004–568$05.00/DOI: http://dx.doi.org/10.2138/am.2012.3973

It is important to elucidate the phase transitions and the structures observed in the $FeTiO_3$ system to constrain the behavior of ABX_3 type compound at ultrahigh pressures.

In this study, we have clarified the phase transitions of $FeTiO_3$ by performing high-pressure and high-temperature in situ X-ray diffraction analysis and transmission electron microscopy observations. We also found a probable structural model for the orthorhombic $FeTi_3O_7$ phase based on a particle swarm optimization simulation of the crystal structure that is not biased by any known structural information (Wang et al. 2010).

Experimental and theoretical method

We used a single crystal of $FeTiO_3$ trigonal ilmenite synthesized by Takei and Kitamura (1978) as the starting material. This single crystal was powdered and mixed with gold as a pressure marker. It was then sandwiched between NaCl pellets with 10–15 μm thickness and loaded into a sample chamber that had been drilled into a rhenium gasket. High pressures were generated using a lever-type diamond-anvil cell with 250 μm flat culet diamonds. The sample was heated by irradiating it from two sides with two 20–30 μm diameter beams from two fiber lasers. Typical heating duration was up to 15 min in our experiment, and the spatial and temporal variations in temperature were within about ±100 K. The pressure at high temperature was determined from the unit-cell volume of gold (Fei et al. 2004). The pressure error was estimated from the uncertainty of the unit-cell parameter of gold and temperature error, which adds up to less than 1.5 GPa. Several samples were prepared without gold and the pressure was obtained from the unit-cell volume of NaCl and the Raman shift of the diamond anvils for Rietveld refinement and ATEM observation, respectively. (Sata et al. 2002: Akahama and Kawamura 2004).

Angle-dispersive X-ray diffraction measurements were conducted in situ at high pressure and high temperature using the BL10XU beamline at SPring-8. This beamline provides a collimated beam (diameter: 15 μm) of monochromatic X-ray radiation (wavelength: 0.41576 Å). X-ray diffraction spectra were recorded using an imaging plate detector and an X-ray CCD camera. The sample-to-detector distance and inclination of the detector were calibrated using a standard material (CeO_2) at 1 atm. Two-dimensional X-ray diffraction images were integrated with respect to 2θ to obtain conventional one-dimensional diffraction profiles using IPAnalyzer and PDindexer software (Seto et al. 2010).

Some of the recovered samples were observed by analytical transmission electron microscopy (ATEM; JEM-2010F, JEOL) using a voltage of 200 kV and an energy-dispersive spectrometer (EDS) at the Institute for Solid State Physics of the University of Tokyo. Quantitative chemical analysis was performed using the experimentally obtained *k*-factors of the Fe/Ti ratio using $FeTiO_3$ ilmenite as a standard, which are correction factors for ATEM-EDS analysis (Cliff and Lorimer 1975).

The initial structural model for orthorhombic $FeTi_3O_7$ at high pressure was estimated by ab initio calculations using the particle swarm optimization technique as implemented in the Crystal Structure Analysis by Particle Swarm Optimization (CALYPSO) software package (Wang et al. 2010), which is available on the web site of the Ma group (http://nlshm-lab.jlu.edu.cn/~calypso.html). This software is designed to search for the structure with the lowest free energy for given external conditions and it can predict the stable structure of a given compound based on only its chemical composition. This methodology has correctly predicted the crystal structures of various systems including elements and compounds, such as the high-pressure structures of Li (Lv et al. 2011) and Bi_2Te_3 (Zhu et al. 2011). In the present study, the variable-cell simulations were performed for $FeTi_3O_7$ with one and two formula units in the simulation cells at 61 GPa.

Rietveld refinement analysis was performed using the RIETAN-FP software (Izumi and Momma 2007), and the refinements were performed for multiphase samples. Peak profiles were fitted with pseudo-Voigt functions for each phase. Throughout the refinement procedure, the isotropic atomic displacement parameters were fixed at 1.0 for all atoms.

Results and discussion

Preliminary ATEM observations were conducted to investigate the decomposition phase assemblage in $FeTiO_3$ at high pressures and high temperatures because ATEM can sensitively detect the decomposition (if there is any). The dissociation to $FeO + FeTi_3O_7$ has been already reported above 40 GPa and 2000 K (Nishio-Hamane et al. 2010b). In the present study, two new decomposition assemblages were found in the recovered samples synthesized at about 35 GPa. Figure 1 shows bright-field transmission images of the samples recovered from 35 GPa. The recovered samples consist of a $FeO + TiO_2$ phase assemblage (sample heated at 1600 K) and a $Fe_2TiO_4 + TiO_2$ phase assemblage (sample heated at 2000 K) (Table 1). A $FeO + FeTi_3O_7$ phase assemblage was also observed in the sample recovered above 40 GPa and high temperature, which is consistent with the results of a previous study (Nishio-Hamane et al. 2010b). No other dissociation was found in the recovered samples synthesized up to 70 GPa at high temperature.

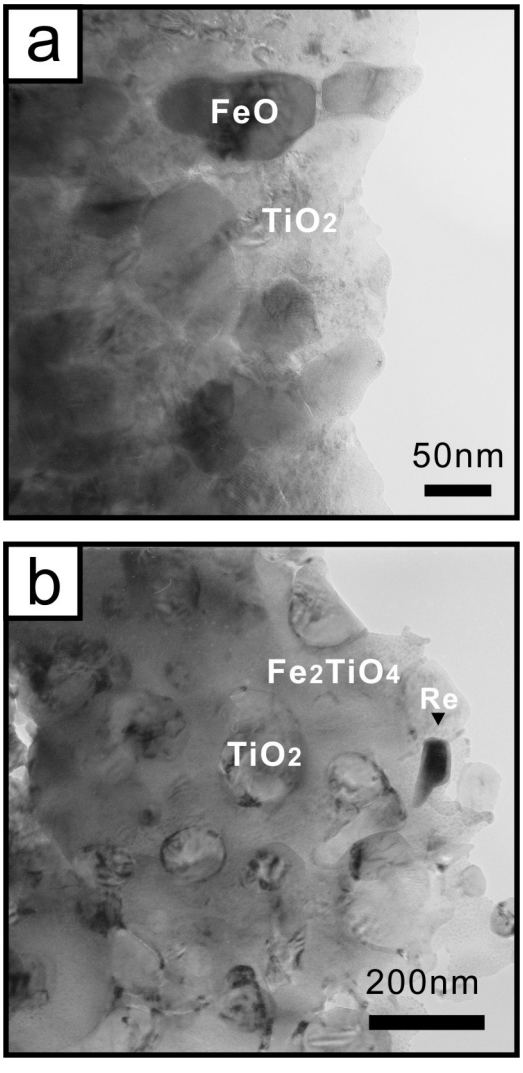

Figure 1. Bright-field transmission electron microscopy images of recovered samples from 35 GPa and (**a**) 1600 and (**b**) 2000 K. Two decomposition assemblages are obtained depending on the synthesis temperature; $FeO + TiO_2$ and $Fe_2TiO_4 + TiO_2$ phase relations are found at 35 GPa and 1600 and 2000 K, respectively. Rhenium (Re) is contamination from the gasket during sample preparation by the ion milling under a low beam angle.

TABLE 1. ATEM-EDS analysis of product phases recovered from 35 GPa and 1600 and 2000 K

	35 GPa and 1600 K		35 GPa and 2000 K	
	FeO	TiO_2	Fe_2TiO_4	TiO_2
TiO_2	1.2(2)	96.1(35)	31.2(13)	95.8(25)
FeO	98.8(20)	3.9(7)	68.8(23)	4.2(5)
Total	100	100	100	100
	O = 1	O = 2	O = 4	O = 2
Ti	0.01	0.98	1.01	0.98
Fe	0.97	0.04	1.98	0.04
Total	0.98	1.02	2.99	1.02

X-ray diffraction measurements were performed in situ at high pressure and temperature to determine the phase relation and the structures of the phases. Figure 2 shows representative X-ray diffraction patterns for the different phases. The ilmenite phase was still stable at 18 GPa and 1790 K (Fig. 2a), while it transformed into orthorhombic perovskite at 25 GPa and 1610 K (Fig. 2b). Although we observed the perovskite phase at 38 GPa at room temperature in the previous work (Nishio-Hamane et al. 2010b), the X-ray diffraction patterns changed and many diffraction peaks appeared at 34–40 GPa when heated to 1440–1990 K. The results of these preliminary ATEM observations assist in indexing the phases. The diffraction peaks obtained at 34 GPa and 1990 K (Fig. 2c) can be indexed as the orthorhombic $CaTi_2O_4$-type Fe_2TiO_4 (Yamanaka et al. 2009) and the orthorhombic OI-type TiO_2 (Dubrovinskaia et al. 2001; Nishio-Hamane et al. 2010b). Cubic B1-type wüstite together with the OI phase appeared instead of Fe_2TiO_4 at 40 GPa and 1440 K (Fig. 2d), which is consistent with ATEM observations. We also confirmed that $CaTi_2O_4$-type Fe_2TiO_4 was quenchable and that OI-type TiO_2 reverted to the α-PbO_2 phase under ambient conditions. Finally, we observed an assemblage of wüstite and orthorhombic $FeTi_3O_7$ at 54 GPa and 2360 K (Fig. 2e). The latter phase became amorphous on releasing the pressure, which is consistent with a previous study (Nishio-Hamane et al. 2010b).

Figure 3 summarizes the high-pressure and high-temperature phase relation in $FeTiO_3$ determined by the present study. A theoretical study predicted the $CaIrO_3$-type phase and an assemblage of wüstite and TiO_2 cotunnite phases (Wilson et al. 2005). However, these phases were not observed at high pressures and high temperatures in the present experimental study. Five phase assemblages were detected in the phase diagram of $FeTiO_3$ up to 74 GPa and 2600 K; these phases consist of ilmenite, perovskite, 1/2 Fe_2TiO_4 ($CaTi_2O_4$-type) + 1/2 TiO_2 (OI-type), FeO (wüstite) + TiO_2 (OI), and 2/3 FeO (wüstite) + 1/3 $FeTi_3O_7$ (orthorhombic phase). The ilmenite–perovskite boundary lies around 20 GPa, and perovskite was stable up to 30 GPa. Between 30 and 44 GPa, Fe_2TiO_4 + OI were observed at high temperatures, whereas wüstite was observed instead of Fe_2TiO_4 at low temperatures. The boundary was a positive dP/dT slope, and it can be approximately described as linear: P (GPa) = 0.025 T (K) – 3.75. Wüstite + $FeTi_3O_7$ appeared above 44 GPa and was stable up to 74 GPa and high temperature.

At 61 GPa and 300 K (after heating at 2000 K), X-ray diffraction shows rhombohedral wüstite and orthorhombic $FeTi_3O_7$ phases (Fig. 4). The orthorhombic $FeTi_3O_7$ phase can be indexed by the $I222$, $I2_12_12_1$, $Imm2$, and $Immm$ space groups with $Z = 2$ in the unit cell (Nishio-Hamane et al. 2010b), but its structure has not yet been determined. We used the CALYPSO software

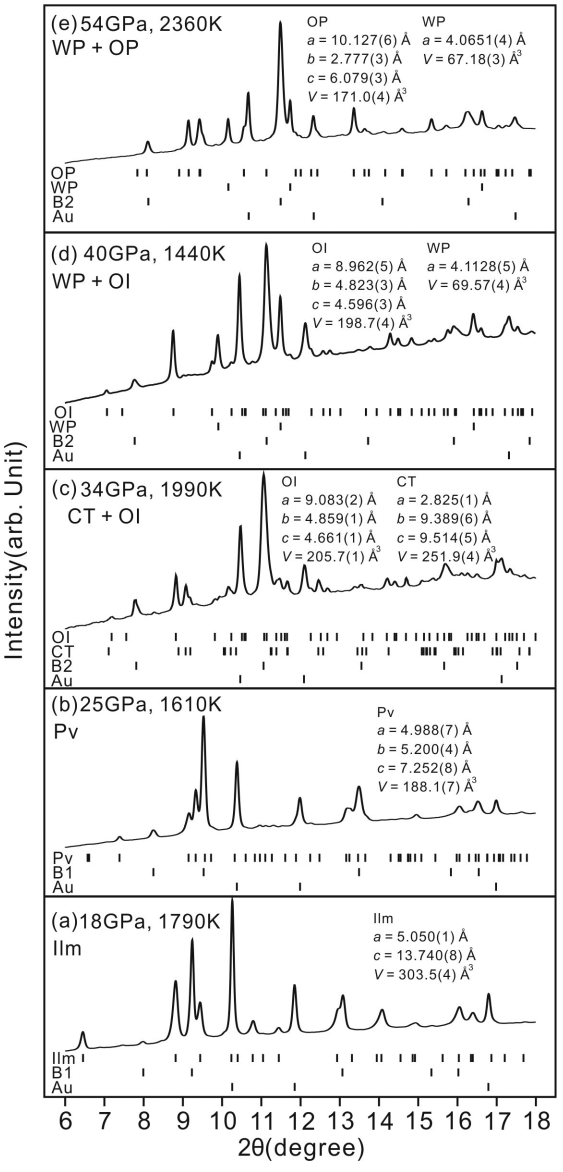

FIGURE 2. Representative X-ray diffraction pattern for $FeTiO_3$ at high pressure and high temperature. (**a**) $FeTiO_3$ ilmenite transformed into (**b**) perovskite, (**c**) $CaTi_2O_4$-type Fe_2TiO_4 and OI-type TiO_2, (**d**) wüstite and OI, and (**e**) wüstite and orthorhombic $FeTi_3O_7$ with increasing pressure. Au = gold; B1 = B1-type NaCl; B2 = B2-type NaCl; CT = $CaTi_2O_4$-type Fe_2TiO_4; Ilm = ilmenite; OI = OI-type TiO_2; OP = orthorhombic $FeTi_3O_7$; Pv = perovskite; WP = wüstite. Bars below X-ray diffraction patterns indicate the peak positions calculated from the unit-cell parameters determined for each phase. The insets give the unit-cell parameters of the product phases at high pressure and high temperature.

package (Wang et al. 2010) to obtain the structural model for orthorhombic $FeTi_3O_7$. Independent particle swarm optimization simulations with input parameters of pressure of 61 GPa and chemical composition of O:Ti:Fe = 7:3:1 predicted the orthorhombic structure of $Imm2$ space group with $Z = 2$, which had not been previously determined. These blindly predicted space group and Z number are quite consistent with the experimental results and thus Rietveld refinement was performed to check the

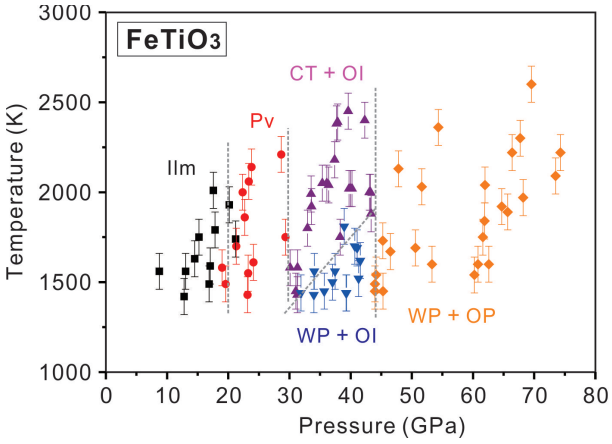

FIGURE 3. Phase diagram for $FeTiO_3$ at high pressure and high temperature determined by in situ X-ray diffraction measurements. CT = $CaTi_2O_4$-type Fe_2TiO_4; Ilm = ilmenite; OI = OI-type TiO_2; OP = orthorhombic $FeTi_3O_7$; Pv = perovskite; WP = wüstite. (Color online.)

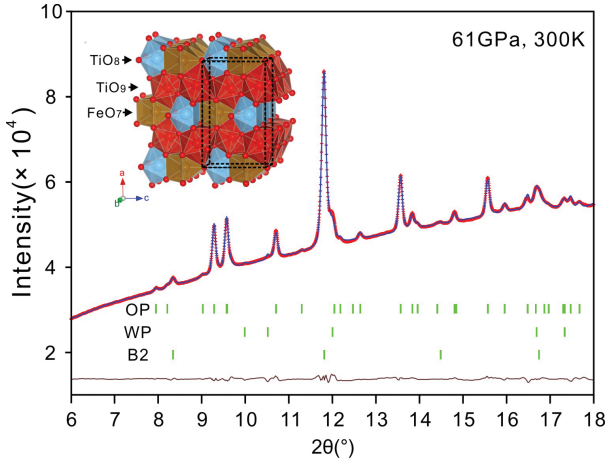

FIGURE 4. Observed X-ray diffraction pattern of orthorhombic $FeTi_3O_7$ (OP) with rhombohedral wüstite (WP) and B2-type NaCl (B2) at 61 GPa and 300 K (dots) with calculated profile of *Imm*2 model (curve) after Rietveld refinement. The ticks indicate the calculated peak positions for each phase. The differences between the observed and calculated profiles are shown below the ticks. The final fit resulted in reliability factors of R_{wp} = 0.47%, R_p = 0.35%, and R_p (without background) = 10.14%. Here $R_{wp} = [\Sigma iwi\{yi - fi(x)\}^2/\Sigma iwiy^2]^{1/2}$ and $R_p = \Sigma i|yi - fi(x)|/\Sigma iyi$ are R factors, where yi is the observed intensity at step i, $fi(x)$ is the calculated intensity, and wi is the weight. Inset shows the $FeTi_3O_7$ structure, which consists of polyhedra of monocapped FeO_7 prisms, bicapped TiO_8 prisms, and tricapped TiO_9 prisms. (Color online.)

validity of the predicted structure. Figure 4 shows the observed X-ray diffraction pattern and the calculated profile based on the *Imm*2 model after Rietveld refinement. Rietveld refinement converged and yielded R_{wp} = 0.47%, R_p = 0.35%, and R_p (without background) = 10.14%. Table 2 lists the structural parameters obtained and the inset of Figure 4 shows the crystal structure obtained using the VESTA program (Momma and Izumi 2008). The determined structure of $FeTi_3O_7$ consists of the polyhedra for monocapped prism FeO_7, bicapped prism TiO_8, and tricapped prism TiO_9. They form a laminated structure by producing a layer of FeO_7 and TiO_8 polyhedra and a TiO_9 polyhedral layer, which develop on the **b-c** plane and stack along the **a** axis. The AB_3X_7-type oxide compound has been scarcely known even at ambient pressure (e.g., Wyckoff 1965), and no compound has been reported that decomposes into several phases containing such composition under pressure. Moreover, so far we could not find any other compounds that have structure similar to that reported in the present $FeTi_3O_7$.

A series of ATEM observations and in situ X-ray diffraction measurements at high pressure and high temperature revealed various phase relations in $FeTiO_3$. Figure 5 shows the molar volumes of the phases in $FeTiO_3$. As shown in Figure 3, the high-pressure transition sequence in $FeTiO_3$ is concluded to be ilmenite → perovskite → Fe_2TiO_4 + OI → wüstite + OI → wüstite + $FeTi_3O_7$ around 1500–1800 K isotherm. At room temperature, the volume decreases by about 5.3% for ilmenite to perovskite, 2.5% to Fe_2TiO_4 + OI, 1.7% to wüstite + OI, and 4.1% to wüstite + $FeTi_3O_7$ around the transition pressures. As we can see from these relations the assemblage of wüstite + $FeTi_3O_7$ has extremely high efficiency of packing and is denser than the hypothetical assemblage of wüstite + cotunnite TiO_2 calculated from its equation of state (Jacobsen et al. 2005; Nishio-Hamane et al. 2010a). So far, the possibility of the decomposition containing

TABLE 2. Atomic coordinates of $FeTi_3O_7$ with *Imm*2 symmetry at 61 GPa and 300 K after refinement

Site	*x*	*y*	*z*
Fe1	0	0	0.665(1)
Ti1	0	0.5	0.205(2)
Ti2	0.2328(3)	0	0.896(2)
O1	0	0	−0.013(4)
O2	0.3013(8)	0	0.607(3)
O3	0.651(1)	0	0.223(2)
O4	0.885(1)	0	0.386(2)

Note: a = 9.9522(5), b = 2.7397(1), c = 5.9953(2) Å, and V = 163.47(1) Å^3.

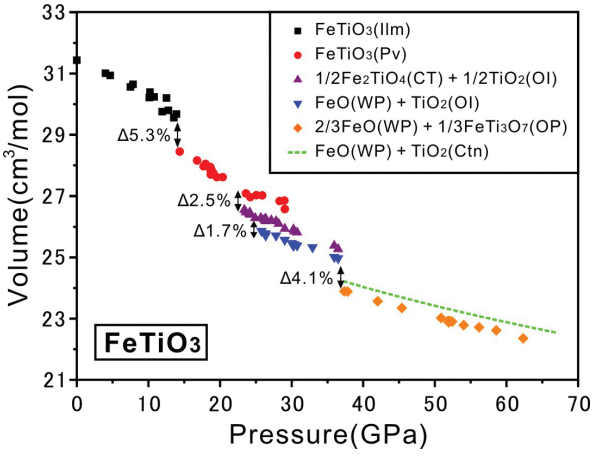

FIGURE 5. Pressure dependence of the volume of the high-pressure phase assemblage in $FeTiO_3$ at 300 K. FeO (WP) + TiO_2 (Ctn) is the hypothetical assemblage calculated using the equation of state for each phase (Jacobsen et al. 2005; Nishio-Hamane et al. 2010b). The pressure and volume error is shown within the symbols size. CT = $CaTi_2O_4$-type Fe_2TiO_4; Ctn = cotunnite-type TiO_2; Ilm = ilmenite; OI = OI-type TiO_2; OP = orthorhombic $FeTi_3O_7$; Pv = perovskite; WP = wüstite. (Color online.)

such oxide had not been considered at all. This new phase relation provides an important model for constraining the behavior for ABX_3 compounds at ultrahigh pressures such as the states of $MgSiO_3$ and $CaSiO_3$, which may be major components of the deep interiors of giant planets. First-principles density functional theory calculations predict that $MgSiO_3$ and $CaSiO_3$ decompose into the B2-type monoxide + cotunnite SiO_2 at sub-terapascal pressures (Umemoto et al. 2006a; Umemoto and Wenzcovitch 2006; Tsuchiya and Tsuchiya 2011). However, our experimental results suggest that the AB_3X_7-type oxide instead of cotunnite SiO_2 may produce the denser assemblage even in the silicate system. The discrepancy between the theoretical prediction and the experiment for the high-pressure behavior of ABX_3 has been also found in $NaMgF_3$, which is analog material for $MgSiO_3$ (Umemoto et al. 2006b; Grocholski et al. 2010) Our new model has not yet been proposed as a candidate, but our suggestion will be important for predicting the mineral assemblage in the deep interiors of giant planets.

Acknowledgments

High-pressure and high-temperature in situ X-ray experiments were conducted at SPring-8 (BL10XU beamline) under the auspices of proposals 2010B1526. This work was supported by a Grant-in-Aid for Research Activity Start-up (Grant no. 22840017) and Young Scientists B (Grant no. 23740389) from the Japan Society for the Promotion of Science. M.Z. and Y.M. thank the National Natural Science Foundation of China for financial support (Grant no. 11025418).

References cited

Akahama, Y. and Kawamura, H. (2004) High-pressure Raman spectroscopy of diamond anvils to 250 GPa: method for pressure determination in the multimegabar pressure range. Journal of Applied Physics, 96, 3748–3751.

Cliff, G. and Lorimer, G.W. (1975) Quantitative-analysis of thin specimens. Journal of Microscopy, 103, 203–207.

Dubrovinskaia, N.A., Dubrovinsky, L.S., Ahuja, R., Prokopenko, V.B., Dmitriev, V., Weber, H.P., Osorio-Guillen, J.M., and Johansson, B. (2001) Experimental and theoretical identification of a new high-pressure TiO_2 polymorph. Physical Review Letters, 87, 27550.

Fei, Y., Li, J., Hirose, K., Minarik, W., Orman, J.V., Sanloup, C., van Westrenen, W., Komabayashi, T., and Funakoshi, K. (2004) A critical evaluation of pressure scales at high temperatures by in situ X-ray diffraction measurements. Physics of the Earth and Planetary Interiors, 143–144, 515–526.

Grocholski, B., Shim, S.-H., and Prakapenka, V.B. (2010) Stability of the $MgSiO_3$ analog $NaMgF_3$ and its implication for mantle structure in super-Earth. Geophysical Research Letters, 37, L14204.

Izumi, F. and Momma, K. (2007) Three-dimensional visualization in powder diffraction. Solid State Phenomena, 130, 15–20.

Jacobsen, S.D., Lin, J., Angel, R.J., Shen, G., Prakapenka, V.B., Dera, P., Mao, H., and Hemley, R.J. (2005) Single-crystal synchrotron X-ray diffraction study of wüstite and magnesiowüstite at lower-mantle pressures. Synchrotron Radiation, 12, 557–583.

Leinenweber, K., Utsumi, W., Tsuchida, Y., Yagi, T., and Kurita, K. (1991) Unquenchable high-pressure perovskite polymorphs of $MnSnO_3$ and $FeTiO_3$. Physics and Chemistry of Minerals, 18, 244–250.

Lv, J., Wang, Y., Zhu, L., and Ma, Y. (2011) Predicted Novel High-Pressure Phases of Lithium. Physical Review Letters, 106, 015503.

Momma, K. and Izumi, F. (2008) VESTA: a three-dimensional visualization system for electronic and structural analysis. Journal of Applied Crystallography, 41, 653–658.

Murakami, M., Hirose, K., Kawamura, K., Sata, N., and Ohishi, Y. (2004) Post-perovskite phase transition in $MgSiO_3$. Science, 304, 855–858.

Nishio-Hamane, D., Katagiri, M., Niwa, K., Sano-Furukawa, A., Okada, T., and Yagi, T. (2009) A new high-pressure polymorph of Ti_2O_3: implication for high-pressure phase transition in sesquioxides. High Pressure Research, 29, 379–388.

Nishio-Hamane, D., Shimizu, A., Nakahira, R., Niwa, K., Sano-Furukawa, A., Okada, T., Yagi, T., and Kikegawa, T. (2010a) The stability and equation of state for cotunnite phase of TiO_2 up to 70 GPa. Physics and Chemistry of Minerals, 37, 129–136.

Nishio-Hamane, D., Yagi, T., Ohshiro, M., Niwa, K., Okada, T., and Seto, Y. (2010b) Decomposition of perovskite $FeTiO_3$ into wüstite $Fe_{1-x}Ti_{0.5x}O$ and $FeTi_3O_7$ at high pressure. Physical Review B, 82, 092103.

Oganov, A.R. and Ono, S. (2004) Theoretical and experimental evidence for a post-perovskite phase of $MgSiO_3$ in the Earth's D" layer. Nature, 430, 445–448.

Okada, T., Yagi, T., and Nishio-Hamane, D. (2011) High-pressure phase behavior of $MnTiO_3$: decomposition of perovskite into MnO and $MnTi_2O_5$. Physics and Chemistry of Minerals, 38, 251–258.

Sata, N., Shen, G., Rivers, M.L., and Sutton, S.R. (2002) Pressure-volume equation of state of the high-pressure B2 phase of NaCl. Physical Review B, 65, 104114.

Seto, Y., Nishio-Hamane, D., Nagai, T., and Sata, N. (2010) Development of a software suite on X-ray diffraction experiments. The Review of High Pressure Science and Technology, 20, 269–276.

Takei, H. and Kitamura, K. (1978) Growth of $FeTiO_3$ (ilmenite) crystals by floating-zone method. Journal of Crystal Growth, 44, 629–631.

Tsuchiya, T. and Tsuchiya, J. (2011) Prediction of a hexagonal SiO_2 phase affecting stabilities of $MgSiO_3$ and $CaSiO_3$ at multimegabar pressures. Proceedings of National Academy of Science, 108, 1252–1255.

Umemoto, K. and Wenzcovitch, R.M. (2006) Potential ultrahigh pressure polymorphs of ABX_3-type compounds. Physical Review B, 74, 224105.

——— (2008) Prediction of an U_2S_3-type polymorph of Al_2O_3 at 3.7 Mbar. Proceedings of National Academy of Science, 105, 6526–6530.

Umemoto, K., Wenzcovitch, R.M., and Allen, P.B. (2006a) Dissociation of $MgSiO_3$ in the cores of gas giants and terrestrial exoplanes. Science, 311, 983–986.

Umemoto, K., Wenzcovitch, R.M., Weidner, D.J., and Parise, J.B. (2006b) $NaMgF_3$: A low-pressure analog of $MgSiO_3$, Geophysical Research Letters, 33, L15304.

Wang, Y., Lv, J., Zhu, L., and Ma, Y. (2010) Crystal structure prediction via particle-swarm optimization. Physical Review B, 82, 094116.

Wilson, N.C., Russo, S.P., Muscat, J., and Harrison, N.M. (2005) High-pressure phase of $FeTiO_3$ from first principles. Physical Review B, 72, 024110.

Wu, X., Steinle-Neumann, G., Narygina, O., McCammon, C., Pascarelli, S., Aquilanti, G., Prakapenka, V., and Dubrovinsky, L. (2009a) Iron oxidation state of $FeTiO_3$ under high pressure. Physical Review B, 79, 094106.

Wu, X., Steinle-Neumann, G., Narygina, O., Kantor, I., McCammon, C., Prakapenka, V., Swamy, V., and Dubrovinsky, L. (2009b) High pressure behavior of perovskite: $FeTiO_3$ dissociation into $(Fe_{1-\delta},Ti_\delta)O$ and $Fe_{1+\delta}Ti_{2-\delta}O_5$. Physical Review Letters, 103, 065503.

Wyckoff, R.W.G. (1965) Crystal structures, 2nd ed., Inorganic Compounds $R_x(MX_4)_y$,$R_x(M_nX_p)_y$, Hydrates and Ammoniates, vol. 3. Wiley, New York.

Zhu, L., Wang, H., Wang, Y., Lv, J., Ma, Y., Cui, Q., Ma, Y., and Zou, G. (2011) Substitutional alloy of Bi and Te at High Pressure. Physical Review Letters, 106, 145501.

Yamanaka, T., Mine, T., Asogawa, S., and Nakamoto, Y. (2009) Jan-Teller transition of Fe_2TiO_4 observed by maximum entropy method at high pressure and low temperature. Physical Review B, 80, 134120.

Yusa, H., Tsuchiya, T., Tsuchiya, J., Sata, N., and Ohishi, Y. (2008) α-Gd_2S_3-type structure in In_2O_3: Experiments and theoretical confirmation of a high-pressure polymorph in sesquioxide. Physical Review B, 78, 092107.

Manuscript received August 15, 2011
Manuscript accepted November 14, 2011
Manuscript handled by Sergio Speziale